How to cite: *Angew. Chem. Int. Ed.* **2023**, *62*, e202311983
doi.org/10.1002/anie.202311983

Artificial Intelligence and MOFs | Hot Paper

A GPT-4 Reticular Chemist for Guiding MOF Discovery**

*Zhiling Zheng[+], Zichao Rong[+], Nakul Rampal, Christian Borgs, Jennifer T. Chayes, and Omar M. Yaghi**

Abstract: We present a new framework integrating the AI model GPT-4 into the iterative process of reticular chemistry experimentation, leveraging a cooperative workflow of interaction between AI and a human researcher. This GPT-4 Reticular Chemist is an integrated system composed of three phases. Each of these utilizes GPT-4 in various capacities, wherein GPT-4 provides detailed instructions for chemical experimentation and the human provides feedback on the experimental outcomes, including both success and failures, for the in-context learning of AI in the next iteration. This iterative human-AI interaction enabled GPT-4 to learn from the outcomes, much like an experienced chemist, by a prompt-learning strategy. Importantly, the system is based on natural language for both development and operation, eliminating the need for coding skills, and thus, make it accessible to all chemists. Our collaboration with GPT-4 Reticular Chemist guided the discovery of an isoreticular series of MOFs, with each synthesis fine-tuned through iterative feedback and expert suggestions. This workflow presents a potential for broader applications in scientific research by harnessing the capability of large language models like GPT-4 to enhance the feasibility and efficiency of research activities.

Introduction

The advancement of reticular chemistry relies on our ability to expand the repertoire of materials and devise innovative strategies to exploit their properties.[1] The mastery of this chemistry requires working knowledge in various disciplines of chemistry (organic, inorganic, physical, analytical, and computational), physics, biology, as well as material science and engineering.[1c,2] However, training a reticular chemist to such a degree of proficiency is time-intensive, necessitating a comprehensive understanding of project design and workflow, as well as expertise beyond the traditional confines of chemistry. Indeed, the development of this depth and breadth of knowledge is typically acquired over years of education and training. We believe that the emerging field of artificial intelligence (AI) and more specifically large language models (LLMs) like GPT-4 are poised to help bridge the knowledge gap between these disciplines and do so with efficiency and speed.[3]

Implementation of this vision requires the seamless integration of AI models into the day-to-day activities and workflow of a reticular chemist.[4] In the present report, we use GPT-4 as a demonstration of how this could be done. GPT-4, being proficient in language comprehension,[3b,5] can facilitate experiment design,[6] review and summarize research articles,[7] provide educational introductions to various concepts and techniques,[8] and assist in data interpretation[9] when guided by carefully designed prompts with explicit instructions.[3e,5c,10] Yet, as it stands, GPT-4 alone lacks the capability to perform a core component of chemistry—experimentation, which is essentially a series of iterative trial-and-error cycles driven by observations and hypotheses. Here, we show initial steps for integrating GPT-

[*] Prof. Dr. O. M. Yaghi
Department of Chemistry, Kavli Energy Nanoscience Institute, and Bakar Institute of Digital Materials for the Planet, College of Computing, Data Science, and Society, University of California, Berkeley
Berkeley, CA-94720 (United States)
and
KACST—UC Berkeley Center of Excellence for Nanomaterials for Clean Energy Applications, King Abdulaziz City for Science and Technology
Riyadh 11442 (Saudi Arabia)
E-mail: yaghi@berkeley.edu

Z. Zheng,[+] Z. Rong,[+] Dr. N. Rampal
Department of Chemistry, Kavli Energy Nanoscience Institute, and Bakar Institute of Digital Materials for the Planet, College of Computing, Data Science, and Society, University of California, Berkeley
Berkeley, CA-94720 (United States)

Prof. Dr. C. Borgs
Department of Electrical Engineering and Computer Sciences and Bakar Institute of Digital Materials for the Planet, College of Computing, Data Science, and Society, University of California, Berkeley
Berkeley, CA-94720 (United States)

Prof. Dr. J. T. Chayes
Department of Electrical Engineering and Computer Sciences, Department of Statistics, Department of Mathematics, School of Information, and Bakar Institute of Digital Materials for the Planet, College of Computing, Data Science, and Society, University of California, Berkeley
Berkeley, CA-94720 (United States)

[+] These authors contributed equally to this work.

[**] A previous version of this manuscript has been deposited on a preprint server (https://doi.org/10.48550/arXiv.2306.14915).

4 into the iterative process of chemical experimentation and propose a novel framework wherein GPT-4 works in tandem with a human researcher at any expertise level. Our strategy features having GPT-4 provide detailed step-by-step instructions for experiments, and the human researcher carries out these procedures and provides detailed feedback on the observations and results. This iterative in-context learning process allows the GPT-4 Reticular Chemist to have access to the experimental outcomes, thereby enabling it to learn from both successes and failures, just like an experienced chemist. This human-AI interaction loop continues until the project goal is achieved, with GPT-4 dynamically adjusting its strategy based on the outcomes of previous iterations. This innovative approach reaps mutual benefits—GPT-4 Reticular Chemist gains real-world experimental validation of its plans and learns from the outcomes, and the human benefits from accelerated research progress under the professional guidance of GPT-4, akin to having a personalized mentor.

Results and Discussion

We designed a novel prompt learning strategy framework that integrates GPT-4 into reticular chemistry, utilizing human feedback to expedite the discovery of new MOFs. Impressively, this symbiotic human-AI collaboration based on two-way learning process led to the sequential discovery of four isoreticular MOFs bearing the same generic chemical formula of $[Al_3(\mu\text{-}OH)_3(HCOO)_3(BTB\text{-}X)]$ and further defined and elaborated below. Notably, the synthesis of these MOFs and their linkers and the subsequent optimization and characterization were all designed by GPT-4 and executed by the human researcher.

Our developed framework allows the fast adaptation of Large Language Models (LLMs) such as GPT-4 to the realm of reticular chemistry via prompt engineering and in-context learning, driven by human feedback. The process comprises three interlinked phases, each employing GPT-4 as a reticular chemist with varying degrees of interaction with human counterparts through tailored prompts, we termed Reticular ChemScope, Reticular ChemNavigator, and Reticular ChemExecutor, which are illustrated in Figure 1.

The first phase Reticular ChemScope had GPT-4 create a project blueprint based on given inputs, followed by the second phase Reticular ChemNavigator where the GPT-4 suggested tasks and guided progress based on human feedback. Lastly, in the third phase Reticular ChemExecutor, GPT-4 provided detailed task steps and a feedback template, enabling effective task execution and improvement. The detailed design and description of each phase can be found in the Materials and Methods Section (Supporting Information, Section S1). In addition, an interactive prompt refinement strategy was used to enable GPT-4 to self-compose prompts by providing role descriptions and duties, which were then refined through an iterative process of suggesting, testing, and improvement. The final versions of the prompts for all three phases are depicted in Figures S36–S41.

It should be emphasized that the ChemNavigator serves as the heart of the three-phase framework. It is where most of the proposed experiment—human wet lab experiments—feedback loop takes place and serves as the cornerstone of our human-AI interaction research design. Inspired by previous studies on prompt engineering of GPT models,[11] our prompt was designed to include specific elements such as role definition, goal instructions, memory of previous trials, evaluation process, and structured output as three task choices. These elements were included based on our reasoning to ensure that the input information is provided in an explicit way, to store a summarized memory of the previous information, and to make GPT-4′s logic in suggesting tasks more interpretable. Together, they contribute to GPT-4′s reticular chemist behavior, manageability of development process, accumulation of past learning, interpretability and transparency in GPT-4′s decision-making process, and variety of task choices based on available resources or schedules, respectively. Following the proposed task by ChemNavigator, the ChemExecutor then makes a detailed experimental plan for the human.

In particular, each iteration involves a single instance of human-AI conversation. It begins with the human sharing a summary of prior experiments, successes, and failures, which GPT-4 processes as "memory". GPT-4 also considers the most recent task it had recommended in the previous iteration, along with the human's feedback on the outcomes. The central question posed to GPT-4 is how to advance and guide, given the current status of the project, the goal of discovering and studying a new MOF. Hence, even if every time a new dialogue session is initiated, GPT-4 capitalizes on in-context learning from prior interactions, allowing it to pick up from the latest point of progress. Using this information, GPT-4 evaluates the current state of the project, updates its memory to include a description of the last trial and errors, and suggests three potential actions. These actions are all aimed at progressing towards the completion of the current stage. Since the GPT-4 was asked to come up with reasoning behind its suggestions, the human researcher can critically evaluate them. This evaluation aids in selecting a course of action, based not only on its merit but also on the availability of resources, laboratory instruments, and the expertise level of the human researcher. Subsequent to the task's execution, as guided by GPT-4′s instructions, the human documents the observations and summarizes the outcomes. This summary, presented to GPT-4 in textual format, reinforces its in-context learning, assisting it in making more informed decisions in subsequent steps. This iterative process continues until GPT-4 identifies progress indicators that align with the objectives indicated in the current stage's description and provides an explanation (Supporting Information, Section S8). Guided by GPT-4′s suggestions, the human researcher then decides whether to proceed to the next stage or continue refining the current one.

The complete journey of MOF discovery involved the use of GPT-4 Reticular Chemist workflow outlined in Figure 1 and encompasses the creation of four new MOFs (Figure 2a: MOF-521-H, -*o*F, -*m*F, -CH_3) as detailed in

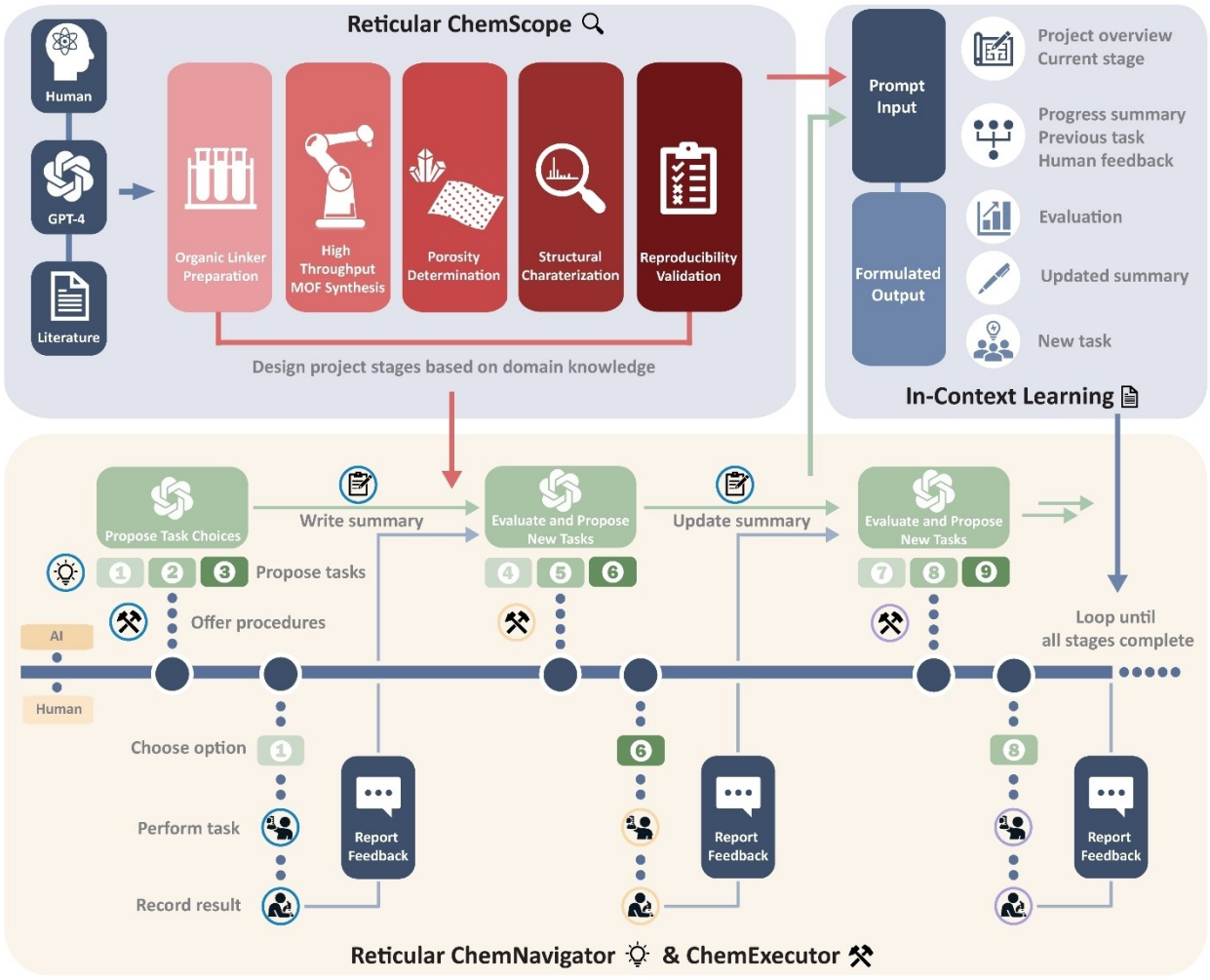

Figure 1. Schematic representation of the GPT-4 based framework functioning as an advanced reticular chemist through strategic prompt engineering and in-context learning informed by human feedback. This GPT-4 Reticular Chemist workflow encapsulates three states: the "Reticular ChemScope", responsible for devising the foundational research project blueprint by dividing it into major domains of activity; the "Reticular ChemNavigator", which assesses the latest activities and presents three potential task options for the human researcher; and the "Reticular ChemExecutor" that furnishes comprehensive procedural guidelines for the selected task, facilitating step-by-step human engagement. All three states are powered by GPT-4 but are given three different types of prompts. The GPT-4's in-context learning capacity is nurtured through a combination of a pre-engineered prompt system and continual human feedback, linked to each task performed. The development and execution of this workflow only require natural language, with no coding involved.

Figures S47–S165, where the input into and the output from GPT-4 are shown. Notably, one of these compounds, MOF-521-H, was previously discovered accidentally as a by-product during the synthesis of MOF-520,[12] another BTB-based aluminum MOF, and remained unpublished. GPT-4 Reticular Chemist, however, unaware of and thus unbiased by the synthesis details from this previous study, independently designed a strategy for these four new MOFs, including MOF-521-H. Interestingly, the optimized synthesis condition established by GPT-4 was subtly different from what humans had previously discovered alone (Supporting Information, Section S2 and Section S9).

Succinctly, upon initiation, the first stage saw Reticular ChemNavigator guiding the human researcher to seek synthesis routes to obtain the linkers, primarily through a thorough literature review (Figures S1–S6). Following a preliminary plan for synthesis, the dialogue directed the human to conduct the organic synthesis reaction, overcome the challenges, and finally confirm the linker by proton NMR (Figures S7–S10). With the linkers in hand, and guiding the human in summarizing the literature search,[13] the second research phase phase focused on identifying the best conditions for MOFs formation, encompassing modifications to metal-linker ratio, temperature, reaction time, modulator(s), and their proportion (Table 1 and Supporting Information, Section S9). Alongside powder X-ray diffraction (PXRD), microscopic observations were used to report the progress. After several rounds of optimization guided by the suggestions of Reticular ChemNavigator, single crystals of all compounds were obtained. Except for MOF-521-CH_3, whose rod-shaped single crystals were too small for single crystal X-ray diffraction (SXRD), the remaining three

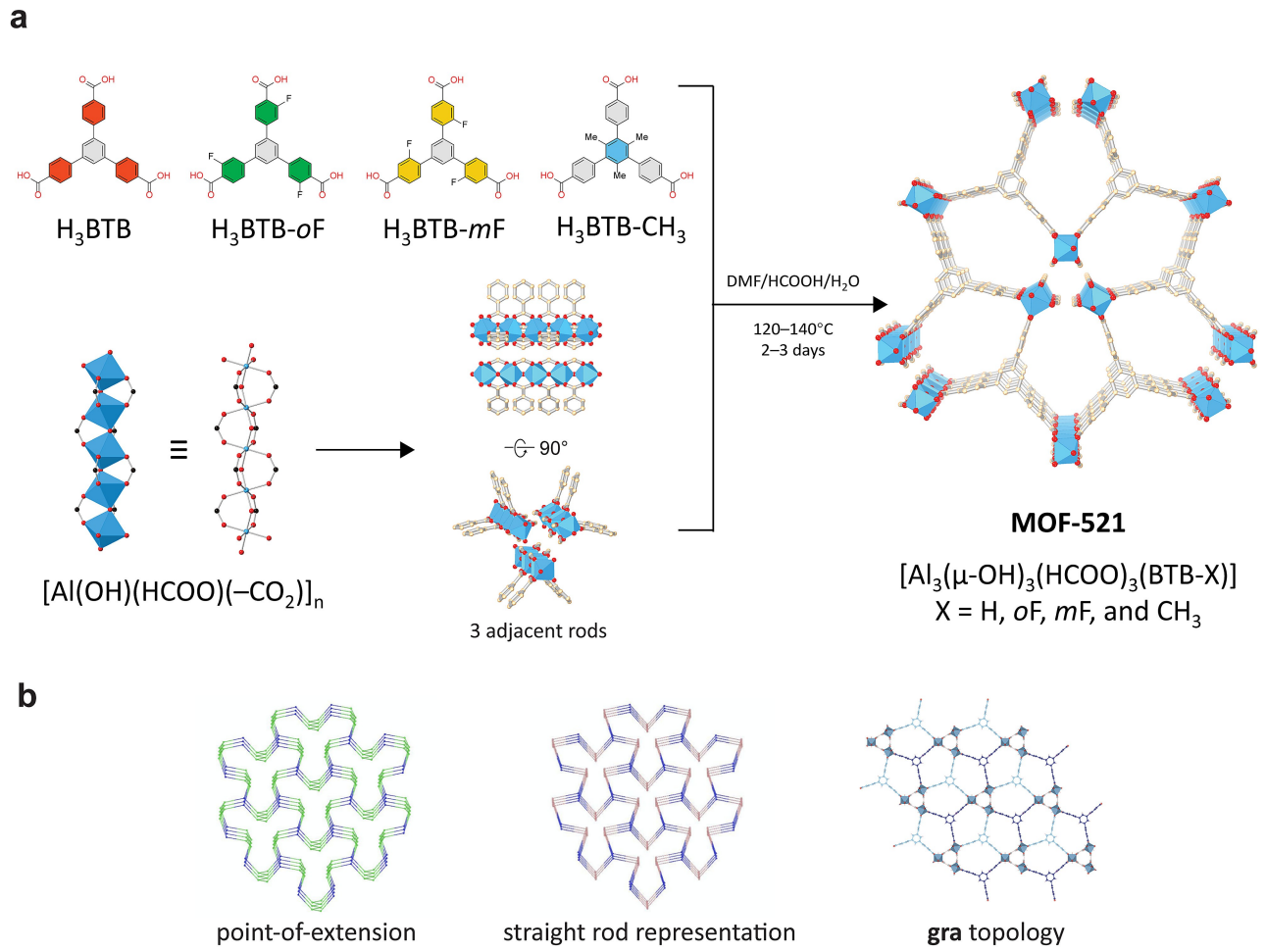

Figure 2. (a) Synthesis and structures of MOF-521. (b) Topological analysis of MOF-521. Color code: Al, blue; O, red; F, green; C, yellow. Hydrogen atoms are omitted for clarity.

compounds were sufficiently large to have their structures characterized by SXRD.[14]

Throughout single crystal X-ray diffraction analysis, it was discovered that the MOF-521 compounds crystallize in the P-62c (No. 190) space group with almost the same unit cell parameters ($a=b=21.9$ Å, $c=6.6$ Å). All MOF-521 compounds are built from rod secondary building units (SBUs): two of the six corners of each AlO_6 octahedron are shared with another two octahedra via μ_2-OH respectively, two corners are bridged by carboxylate from the BTB linker, and the last two corners are capped by formates, thus forming a 1-dimensional straight rod (Figure 2a). There is one μ_2-OH, one carboxylate from the BTB linker and one formate between the two adjacent AlO_6 octahedra. The rods are parallelly connected to each other via BTB linkers, while the μ_2-OH groups point into the large pores and form hydrogen bonding with DMF or water. Positional disorder is found at the peripheral phenyl rings of BTB and can be refined to two symmetric positions. The dihedral angle between the peripheral phenyl ring and the central phenyl ring in MOF-521 (MOF-521-H: 62.9(4)°, MOF-521-*o*F: 51.9-(4)°, and MOF-521-*m*F: 68.0(5)°) is larger than the one in MOF-520[15] (36.4(7)°, 36.7(8)° and 40.8(7)°). Adding functionalities onto the phenyl rings would introduce steric hindrance and therefore larger dihedral angles are favored. In addition, the carboxylate of the BTB is almost coplanar with the peripheral phenyl ring to which it connected so that the large dihedral angle determines the plane of the carboxylate to be perpendicular to the plane of the central phenyl ring and also the formation of rod SBUs.

Given the unique rod packing presented in four MOF-521 compounds, we sought to further examine its topology[16] to determine whether they were unprecedented MOFs. However, the inherently mathematical and analytical nature of this process surpassed GPT-4's capabilities,[3b,e] so this analysis was handled by the human side. Several topological analyses were applied to the MOF-521 structure, aiming to better describe its underlying topology, which include standard method, point-of-extension (PE), point-of-extension & metal (PE&M) and straight rod representation (STR).[17] Among them, we believe PE and STR best extract the topological features as they both simplify the rod shape just based on its connection direction to the BTB linkers, which is a conventional analysis for MOFs with rod SBUs

Table 1: Screening conditions for MOF-521 synthesis guided by the Reticular ChemNavigator through iterative learning and inference processes.

Exp.[a]	Linker	Modulator[b]	L:M Ratio[c]	Temp. [°C]	Time [h]
1	BTB-H	FA	1:1	100	48
17	BTB-H	FA	2:3	140	48
21	BTB-H	FA	4:1	140	48
29	BTB-H	FA	3:4	120	72
32	BTB-H	TFA	3:4	120	72
33	BTB-H	TFA/AA (1:1)	3:4	120	72
35	BTB-H	FA/HCl (1:1)	3:4	120	72
41	BTB-H	FA/H_2O (1:2)	3:4	120	72
46	BTB-H	FA/H_2O (4:1)	3:4	120	84
52	BTB-H	FA/H_2O (4:1)	3:4	140	72
54	BTB-*o*F	FA	2:1	140	48
56	BTB-*o*F	FA/H_2O (1:1)	2:1	140	48
60	BTB-*o*F	FA/H_2O (4:1)	3:4	140	48
63	BTB-*o*F	FA/H_2O (4:1)	3:4	120	48
69	BTB-*o*F	FA/H_2O (4:1)	3:4	120	96
71	BTB-*m*F	FA/H_2O (4:1)	3:4	120	72
73	BTB-*m*F	FA/H_2O (4:1)	3:4	110	72
78	BTB-*m*F	FA/H_2O (4:1)	3:5	120	72
79	BTB-*m*F	FA/H_2O (5:1)	3:4	120	72
82	BTB-CH_3	FA/H_2O (4:1)	3:4	120	48
84	BTB-CH_3	FA/H_2O (4:1)	3:4	130	72
86	BTB-CH_3	FA/H_2O (4:1)	1:2	130	72
91	BTB-CH_3	FA/H_2O (4:1)	3:4	150	72

[a] Experiment ID corresponds to each human-conducted experiment following the guidelines provided by the Reticular ChemNavigator, powered by GPT-4. Initial conditions were derived from a comprehensive literature review. For each iteration, GPT-4 suggests a modification of one parameter (e.g., linker to metal ratio, modulator, temperature, or time). For the sake of conciseness, representative conditions were documented in this table. Please refer to Supporting Information, Table S1 and Section S9, for comprehensive details. It is important to note that GPT-4 does not provide explicit predictions, but instead guides human to analyze PXRD patterns, considers previous success and failures reported by human, infers potential avenues for subsequent steps in MOF screening, and provides suggestions to human. [b] Modulator abbreviations: FA = formic acid; TFA = trifluoroacetic acid; AA = acetic acid. [c] This denotes the molar ratio of linker to metal ions.

(Figure 2b). Both methods result in a $(3\text{-c})_3(3\text{-c})$ 2-nodal net, which is also termed as **etc** according to the Reticular Chemistry Structure Resource (RCSR).[18] We found that this $(3\text{-c})_3(3\text{-c})$ 2-nodal net only has 3 entries recorded in the TOPOS database (GEKCAD: $In_{12}S_{34}Sn_4$; OMABEL: $C_{66}H_{78}B_3Cu_6N_{27}S_9W_3$; XEKJUT: $C_{24}H_{15}Cu_3N_{12}O_3$), which included one inorganic compound and two coordination polymers, suggesting MOF-521 is the first MOF to have this topology.

In addition, we note that even though the underlying topology is the same, the MOF-521 structure still differs strongly from the three entries in TOPOS database in that the 3 rod SBUs in MOF-521 are packed so closely to each other as evidenced by the small distance between the central axis of the rods (6.54 Å). The three rod SBUs are not covalently linked because the formates block the coordination sites of the aluminum metal center. This close parallel packing of rod SBUs has not been observed in other MOFs with rod SBUs. Furthermore, given the uniqueness of its SBU, another way to describe the MOF-521 structure is to view the three closely packed rod SBUs as one pseudo rod SBU since the internal space could not be accessed by any guest molecules, and then the structure has a **gra** topology (Figure 2b).

As we moved forward, GPT-4 and the human found a good agreement between the simulated and experimental PXRD patterns, indicating that all four MOF-521 compounds were constructed under the same topology (Figure 3a). A crucial stage was reached in stage 3 when Reticular ChemNavigator initiated investigations into the permanent porosity of the obtained MOF-521 compounds. It gave useful suggestions on setting up the measurement and interpreting the analysis results. The permanent porosity of the MOF-521 family was confirmed by nitrogen sorption measurements, and the experimentally measured surface area of the four MOFs was consistent with the predictions made by Material Studio (Table 2). All the compounds show the Type I isotherms with no significant accompanied hysteresis, and there is a rough trend based on the relationship between the porosity and the size of the functional groups in the framework for both calculated and experimental data. The least substituted MOF-521-H demonstrates the highest BET surface area of 1696 m^2g^{-1}, and

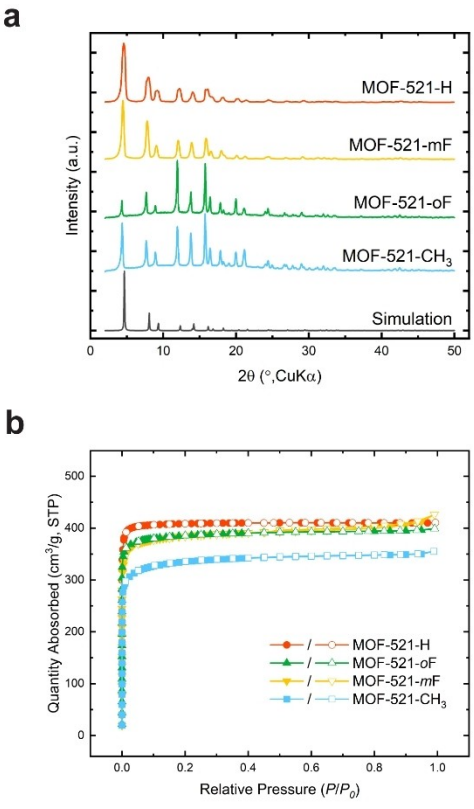

Figure 3. (a) PXRD patterns of MOF-521 compounds. The simulated pattern at the bottom was generated using single crystal structure of MOF-521-H. (b) Adsorption-desorption (filled circles-open circles) isotherms of nitrogen on MOF-521 compounds at a measurement temperature of 77 K.

Table 2: Porosity data for MOF-521 compounds.

Compound	Formula	Crystal Density [g/cm³]	Pore Width [Å]	V_p[a] [cm³/g]	A_{exp}[b] [m²/g]	A_{calc}[b] [m²/g]
MOF-521-H	$Al_3(\mu\text{-}OH)_3(HCOO)_3(C_{27}H_{15}O_6)$	0.851	10.8	0.588	1696	1670
MOF-521-*o*F	$Al_3(\mu\text{-}OH)_3(HCOO)_3(C_{27}H_{12}F_3O_6)$	0.916	10.7	0.564	1562	1540
MOF-521-*m*F	$Al_3(\mu\text{-}OH)_3(HCOO)_3(C_{27}H_{12}F_3O_6)$	0.912	10.9	0.562	1535	1553
MOF-521-CH_3	$Al_3(\mu\text{-}OH)_3(HCOO)_3(C_{30}H_{21}O_6)$	nd[c]	9.3	0.509	1311	1550

[a] V_p is the measured pore volume. [b] A_{exp} and A_{calc} are the experimental measured BET surface area and theoretical geometric surface area, respectively. The calculation was performed on *Materials Studios 8.0* with the N_2 as probe (diameter = 3.681 Å) according to published procedure.[19] [c] nd, no data.

MOF-521-*o*F and MOF-521-*m*F shows a comparable BET surface area of 1535 m^2g^{-1} and 1562 m^2g^{-1}, respectively (Figures S21–S32). On the other hand, the surface area of MOF-521-CH_3 is 1311 m^2g^{-1} and turns to be much lower than other ones, suggesting that the substitution of center benzene has a greater influence on the pore environment and can be potentially used to tune the porosity.

In stage 4, to verify their compositions and chemical formulae, all four MOF-521 compounds underwent proton nuclear magnetic resonance (NMR) spectroscopy and elemental analysis as suggested by the Reticular ChemNavigator. The proton signals from four linkers were assigned based on their chemical shifts and splitting patterns (Figures S11–S14). The DMF solvent peak cannot be identified in the digestion NMR, suggesting that the compounds were fully activated. The appearance of the formate peaks at 8.5 ppm and the linker peak between 6.2 ppm and 7.8 ppm shows good agreement with the chemical formulae of MOF-521 compounds determined by SXRD and elemental analysis. In addition, it further confirms that, instead of moving freely in the pore of the MOF, formates exist as a building ligand on the framework and were not subjected to removal during the activation under vacuum. It's noteworthy that the data analysis was primarily conducted by human intervention, guided by recommendations from GPT-4. The findings were subsequently reported to GPT-4 for further analysis and interpretation, a strategic approach designed to reduce potential hallucination effects from large language model. We note that an experienced chemist may be able to do this without consultation, but the GPT-4 was able to offer three different directions by evaluating the circumstances and help human researcher, especially those who are not so familiar with some of the standard characterization techniques in reticular chemistry, to move on. Next, the thermogravimetric experiment was performed under nitrogen with a heating rate of 5 °C/min. The activated sample demonstrated a two-step weight loss and indicated that almost no solvent or water molecules were present in the pore (Figures S15–S18). We notice that the observed first weight loss between 250–350 °C matches with the weight of the formate ligand (calc. 19.2 %; obs. 20.1 %), and the second step (600–700 °C) can be attributed to the decomposition of the framework.

As shown in Figure 4, the total numbers of prompt iterations are similar across the four MOF-521 compounds. The number of prompt iterations serves as a valuable measure of the efficiency and complexity of the synthesis,

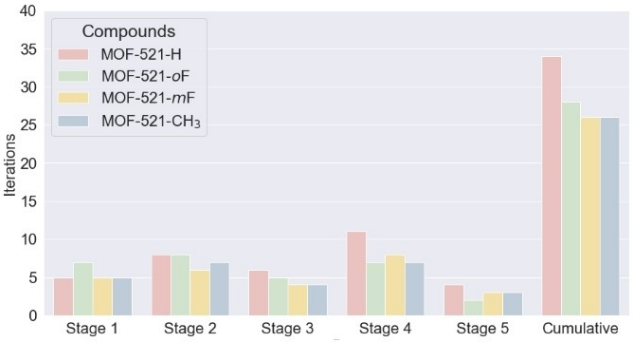

Figure 4. Number of prompting iteration took to complete each stage for the MOF-521 compounds based on BTB-H, BTB-*o*F, BTB-*m*F and BTB-CH_3 linkers. The number of iterations is a function of (i) the human input provided to AI, and (ii) the task picked by the human at each iteration of the approach.

characterization and analysis of each compound. This observation is noteworthy as it underscores the reproducibility and robustness of GPT-4's effectiveness in acting as a reticular chemist to uncover new MOFs. The similarity in iterations across compounds is particularly noteworthy considering that each compound's discovery route differs in aspects such as organic linker preparation, synthesis condition optimization, and property characterization. In this light, the four linkers can be conceptualized as distinct discovery narratives, with each narrative standing as a testament to GPT-4's reproducible efficacy in acting as a reticular chemist for MOF exploration. Moreover, even within identical stages, GPT-4 encountered varied routes. For instance, in the synthesis condition screening phase, one route might prioritize temperature while another emphasizes the metal-to-linker ratio. This flexible approach by GPT-4, adapting and providing tailored suggestions to divergent scenarios, showcases its adeptness at addressing distinct challenges. The consistent number of iterations for each compound suggests that, irrespective of the distinct routes and decisions made, the steps and workload to achieve optimal stage goals remain similar. This consistency underscores GPT-4's ability to avoid situations where it becomes entangled in indecision or ineffective pathways.

Such observations validate not only the method's robustness but also its broader potential applicability for LLM-assisted scientific research. The iterative consistency further ratifies our division into five stages, emphasizing both its logical nature and efficiency. This segmentation, by breaking

down the broader MOF discovery into digestible milestones, mirrors a typical human approach to complex tasks. Such structuring ensures evenly distributed efforts across stages, preventing any one stage from being disproportionately challenging or simple. In the meantime, it is essential to acknowledge that the role of GPT-4 in this research was not simply about discovering the most efficient path, but rather acting as a discerning consultant, providing expert suggestions tailored to researchers at various levels of expertise. As an illustrative point, when juxtaposed against human expert perspectives, over 80 % of GPT-4′s task recommendations were congruent with the immediate challenges faced by researchers and had evidently been taken account into prior project trajectory to ensure the task suggestions are helpful and practical (Table S5). This approach emphasizes a nuanced human-AI collaboration where the AI model serves as a valuable tool to guide and support rather than replace human judgment, reflecting the essence of a symbiotic relationship.

The in-context learning by GPT-4 Reticular Chemist within the system is further evidenced by the observation that the total iteration count for the latter three compounds was less than that for MOF-521-H. This is attributable to the fact that MOF-521-H, being the initial compound, lacked a precedent for guidance. However, once MOF-521-H successfully navigated through all stages, its compiled summary functioned as a directive for subsequent compounds, thereby expediting their processes. In essence, generating a summary based on past successes and failures is analogous to creating a repository of useful tools and guidance that can self-instruct other instances of GPT-4 Reticular Chemist to propose more efficient tasks for the discovery and development of similar MOFs. This reflects the system‘s inherent capability for progressive learning, emphasizing not only the feasibility and efficiency of this approach but also the potential for extending such methods to newcomers and cross-disciplinary researchers.

Conclusion

This research signifies a noteworthy innovation in the traditional conduct of chemical experimentation, bridging the gap between AI and reticular chemistry by integrating the large language model, GPT-4, into the iterative chemical experimentation process. The developed framework emphasizes a symbiotic human-AI collaboration, facilitating research on the synthesis and characterization of new MOFs, as demonstrated by the four isoreticular MOFs. Our findings also underline the value of GPT-4′s guidance across various stages of discovery, including areas that may appear similar in synthesis strategy or optimal conditions. The nuanced guidance provided by the model helps in interpreting the results more effectively and fine-tuning the specific conditions, even where similarities exist. This approach showcases the model‘s potential for scalable application in various scientific fields, adding to its unique contributions.

Moreover, the segmentation of this framework into three interactive phases underpins a manageable, systematic approach to material discovery, laying a foundation towards a visionary goal: the full automation and robotization of the experimental steps via automatic data mining[20] and high-throughput experiments.[21] Moreover, the progressive learning capability embedded within the system showcases the model‘s potential for scalable application in various scientific fields. Ultimately, this work serves as a pioneering step in the convergence of AI and reticular chemistry, opening new possibilities for future scientific discovery. It also serves as a testament to the constructive role of AI in driving scientific research by providing valuable insights and directions, akin to what a human mentor or collaborator might offer in a research setting.

Acknowledgements

Z.Z. would like to extend special gratitude to Jiayi Weng from OpenAI for inspiring discussions on harnessing the potential of GPT-4. We appreciate the guidance from Drs. Xiaokun Pei, Ha Lac Nguyen, and Chuanshuai Li of the Yaghi Lab, Prof. Davide Proserpio, and Prof. Michael O′Keeffe, who provided insightful discussions on the topology of the new MOFs. We also acknowledge the financial support from the Defense Advanced Research Projects Agency (DARPA) under contract HR0011-21-C-0020 and the Bakar Institute of Digital Materials for the Planet (BIDMaP). We also thank the NIH (Grant S10-RR027172) for financial support of the X-ray crystallographic facility at UC Berkeley, and Dr. Nicholas Settineri for the support on using the facility. This research used resources of beamline 12.2.1 at the Advanced Light Source, which is a DOE Office of Science User Facility under contract no. DE-AC02-4105CH11231. In addition, Z.Z. is grateful for the financial support received through a Kavli ENSI Graduate Student Fellowship.

Conflict of Interest

The authors declare no conflict of interest.

Data Availability Statement

The data that support the findings of this study are available in the supplementary material of this article.

Keywords: Artificial Intelligence · Crystals · Large Language Model · Metal–Organic Frameworks · Synthesis

[1] a) O. M. Yaghi, M. J. Kalmutzki, C. S. Diercks, *Introduction to reticular chemistry: metal–organic frameworks and covalent organic frameworks*, John Wiley & Sons, Hoboken, **2019**; b) O. M. Yaghi, M. O′Keeffe, N. W. Ockwig, H. K. Chae, M. Eddaoudi, J. Kim, *Nature* **2003**, *423*, 705–714; c) R. Freund, S. Canossa, S. M. Cohen, W. Yan, H. Deng, V. Guillerm, M.

Eddaoudi, D. G. Madden, D. Fairen-Jimenez, H. Lyu, *Angew. Chem. Int. Ed.* **2021**, *60*, 23946–23974.
[2] C. Gropp, S. Canossa, S. Wuttke, F. Gándara, Q. Li, L. Gagliardi, O. M. Yaghi, *ACS Cent. Sci.* **2020**, *6*, 1255.
[3] a) OpenAI, *arXiv preprint* **2023**, https://doi.org/10.48550/arXiv.2303.08774; b) S. Bubeck, V. Chandrasekaran, R. Eldan, J. Gehrke, E. Horvitz, E. Kamar, P. Lee, Y. T. Lee, Y. Li, S. Lundberg, *arXiv preprint* **2023**, https://doi.org/10.48550/arXiv.2303.12712; c) T. Hope, D. Downey, D. S. Weld, O. Etzioni, E. Horvitz, *Commun. ACM* **2023**, *66*, 62–73; d) H. Wang, T. Fu, Y. Du, W. Gao, K. Huang, Z. Liu, P. Chandak, S. Liu, P. Van Katwyk, A. Deac, *Nature* **2023**, *620*, 47–60; e) Y. Liu, T. Han, S. Ma, J. Zhang, Y. Yang, J. Tian, H. He, A. Li, M. He, Z. Liu, *arXiv preprint* **2023**, https://doi.org/10.48550/arXiv.2304.01852; f) A. D. White, *Nat. Chem. Rev.* **2023**, *7*, 457–458.
[4] H. Lyu, Z. Ji, S. Wuttke, O. M. Yaghi, *Chem* **2020**, *6*, 2219–2241.
[5] a) A. Vaswani, N. Shazeer, N. Parmar, J. Uszkoreit, L. Jones, A. N. Gomez, Ł. Kaiser, I. Polosukhin, *NIPS* **2017**, *30*; b) C. M. Castro Nascimento, A. S. Pimentel, *J. Chem. Inf. Model.* **2023**, *63*, 1649–1655; c) A. M. Bran, S. Cox, A. D. White, P. Schwaller, *arXiv preprint* **2023**, https://doi.org/10.48550/arXiv.2304.05376.
[6] a) Z. Yang, Y. Wang, L. Zhang, *bioRxiv preprint* **2023**, https://doi.org/10.1101/2023.04.19.537579; b) M. M. Rahman, H. J. Terano, M. N. Rahman, A. Salamzadeh, M. S. Rahaman, *J. Educ. Manage. Studies* **2023**, *3*, https://doi.org/10.52631/jemds.v3i1.175.
[7] a) Z. Zheng, O. Zhang, C. Borgs, J. T. Chayes, O. M. Yaghi, *J. Am. Chem. Soc.* **2023**, *145*, 18048–18062; b) S. Wang, H. Scells, B. Koopman, G. Zuccon, *arXiv preprint* **2023**, https://doi.org/10.48550/arXiv.2302.03495.
[8] a) T. M. Clark, *J. Chem. Educ.* **2023**, *100*, 1905–1916; b) K. Hatakeyama-Sato, N. Yamane, Y. Igarashi, Y. Nabae, T. Hayakawa, *ChemRxiv preprint* **2023**, https://doi.org/10.26434/chemrxiv-2023-s1x5p; c) S. Fergus, M. Botha, M. Ostovar, *J. Chem. Educ.* **2023**, *100*, 1672–1675; d) R. P. d. Santos, *arXiv preprint* **2023**, https://doi.org/10.48550/arXiv.2305.11890; e) J.-P. Vert, *Nat. Biotechnol.* **2023**, *41*, 750–751.
[9] a) Y. Kang, J. Kim, *arXiv preprint* **2023**, https://doi.org/10.48550/arXiv.2308.01423; b) D. Noever, F. McKee, *arXiv preprint* **2023**, https://doi.org/10.48550/arXiv.2301.13382.
[10] a) A. G. Parameswaran, S. Shankar, P. Asawa, N. Jain, Y. Wang, *arXiv preprint* **2023**, https://doi.org/10.48550/arXiv.2308.03854; b) Y. Zhou, A. I. Muresanu, Z. Han, K. Paster, S. Pitis, H. Chan, J. Ba, *arXiv preprint* **2022**, https://doi.org/10.48550/arXiv.2211.01910; c) J. White, Q. Fu, S. Hays, M. Sandborn, C. Olea, H. Gilbert, A. Elnashar, J. Spencer-Smith, D. C. Schmidt, *arXiv preprint* **2023**, https://doi.org/10.48550/arXiv.2302.11382.
[11] a) G. Wang, Y. Xie, Y. Jiang, A. Mandlekar, C. Xiao, Y. Zhu, L. Fan, A. Anandkumar, *arXiv preprint* **2023**, https://doi.org/10.48550/arXiv.2305.16291; b) J. Liu, D. Shen, Y. Zhang, B. Dolan, L. Carin, W. Chen, *arXiv preprint* **2021**, https://doi.org/10.48550/arXiv.2101.06804; c) J. S. Park, J. C. O'Brien, C. J. Cai, M. R. Morris, P. Liang, M. S. Bernstein, *arXiv preprint* **2023**, https://doi.org/10.48550/arXiv.2304.03442; d) W. Zhou, Y. E. Jiang, P. Cui, T. Wang, Z. Xiao, Y. Hou, R. Cotterell, M. Sachan, *arXiv preprint* **2023**, https://doi.org/10.48550/arXiv.2305.13304.
[12] X. Pei, H.-B. Bürgi, E. A. Kapustin, Y. Liu, O. M. Yaghi, *J. Am. Chem. Soc.* **2019**, *141*, 18862–18869.
[13] a) D. Saha, R. Zacharia, L. Lafi, D. Cossement, R. Chahine, *Chem. Eng. J.* **2011**, *171*, 517–525; b) Y. Song, M. Yang, X. Zhang, *Sep. Sci. Technol.* **2022**, *57*, 1521–1534; c) F. Gándara, H. Furukawa, S. Lee, O. M. Yaghi, *J. Am. Chem. Soc.* **2014**, *136*, 5271–5274.
[14] Deposition numbers 2288419 (for MOF-521-H), 2288420 (for MOF-521-*o*F), and 2288418 (for MOF-521-*m*F) contain the supplementary crystallographic data for this paper. These data are provided free of charge by the joint Cambridge Crystallographic Data Centre and Fachinformationszentrum Karlsruhe Access Structures service.
[15] S. Lee, E. A. Kapustin, O. M. Yaghi, *Science* **2016**, *353*, 808–811.
[16] D. J. Tranchemontagne, J. L. Mendoza-Cortés, M. O'keeffe, O. M. Yaghi, *Chem. Soc. Rev.* **2009**, *38*, 1257–1283.
[17] a) F. M. A. Noa, M. Abrahamsson, E. Ahlberg, O. Cheung, C. R. Göb, C. J. McKenzie, L. Öhrström, *Chem* **2021**, *7*, 2491–2512; b) L. S. Xie, E. V. Alexandrov, G. Skorupskii, D. M. Proserpio, M. Dincă, *Chem. Sci.* **2019**, *10*, 8558–8565; c) A. Schoedel, M. Li, D. Li, M. O'Keeffe, O. M. Yaghi, *Chem. Rev.* **2016**, *116*, 12466–12535.
[18] M. O'Keeffe, M. A. Peskov, S. J. Ramsden, O. M. Yaghi, *Acc. Chem. Res.* **2008**, *41*, 1782–1789.
[19] T. Düren, F. Millange, G. Férey, K. S. Walton, R. Q. Snurr, *J. Phys. Chem. C* **2007**, *111*, 15350–15356.
[20] a) Y. Luo, S. Bag, O. Zaremba, A. Cierpka, J. Andreo, S. Wuttke, P. Friederich, M. Tsotsalas, *Angew. Chem. Int. Ed.* **2022**, *61*, e202200242; b) S. Park, B. Kim, S. Choi, P. G. Boyd, B. Smit, J. Kim, *J. Chem. Inf. Model.* **2018**, *58*, 244–251; c) A. Nandy, C. Duan, H. J. Kulik, *J. Am. Chem. Soc.* **2021**, *143*, 17535–17547; d) H. Park, Y. Kang, W. Choe, J. Kim, *J. Chem. Inf. Model.* **2022**, *62*, 1190–1198.
[21] D. A. Boiko, R. MacKnight, G. Gomes, *arXiv preprint* **2023**, https://doi.org/10.48550/arXiv.2304.05332.

Manuscript received: August 16, 2023
Accepted manuscript online: October 5, 2023
Version of record online: October 13, 2023